Composite Graphite−Epoxy Electrodes for In Situ Electrochemistry Coupling with High Resolution NMR

Pollyana Ferreira da Silva, Bruna Ferreira Gomes,* Carlos Manuel Silva Lobo, Marcelo Carmo, Christina Roth, and Luiz Alberto Colnago

ACCESS | Metrics & More | Article Recommendations

ABSTRACT: The in situ coupling between electrochemistry and spectrometric techniques can help in the identification and quantification of the compounds produced and consumed during electrochemical reactions. The combination of electrochemistry with nuclear magnetic resonance is quite attractive in this respect, but it has some challenges to be addressed, namely, the reduction in the quality of the NMR signal when the metallic electrodes are placed close to or in the detection region. Since NMR is not a passive technique, the convective effect of the magnetic force (magnetoelectrolysis), which acts by mixing the solution and increasing the mass transport, has to be considered. In seeking to solve the aforementioned problems, we developed a system of miniaturized electrodes inside a 5 mm NMR tube (outer diameter); the working and counter electrodes were prepared with a mixture of graphite powder and epoxy resin. To investigate the performance of the electrodes, the benzoquinone reduction to hydroquinone and the isopropanol oxidation to acetone were monitored. To monitor the alcohol oxidation reaction, the composite graphite−epoxy electrode (CGEE) surface was modified through platinization. The electrode was efficient for in situ monitoring of the aforementioned reactions, when positioned 1 mm above the detection region of the NMR spectrometer. The magnetoelectrolysis effect acts by stirring the solution and increases the reaction rate of the reduction of benzoquinone, because this reaction is limited by mass transport, while no effect on the reaction rate is observed for the isopropanol oxidation reaction.
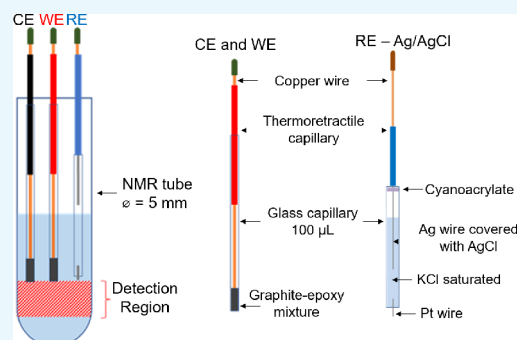
INTRODUCTION

The coupling of electrochemistry with nuclear magnetic resonance (NMR) has been attracting the attention of the scientific community in recent decades due to the possibility of detecting the formation and consumption of species, in real time, which can be used to study reaction mechanisms and kinetics. There are a few dozen models of miniaturized cells that aim to minimize the effects resulting from interference between the techniques, since the placement of electrodes close to or in the NMR detection region can degrade the NMR signal by introducing noise and increasing the width of the peaks.[1−19] Furthermore, when performing the electrochemistry−NMR coupling, it is important to keep in mind the existence of the magnetoelectrolysis effect, where the magnetic field force, F_B,[a] plays a major role, as it originates from the interaction between the magnetic field, B, and the ion flow density, j, as the charged species move through the solution toward the electrode surface, as shown in eq 1.[19−27] This convection force, also termed the magnetohydrodynamic force, stirs the solution with an intensity proportional to the intensity of B; therefore, the greater the intensity of the magnetic field, the greater the agitation caused in the system. For systems that are limited by mass transport, this effect is very evident, as it

significantly increases the reaction rate.[19,28−33] By placing electrodes above the NMR detection region and by taking advantage of the aforementioned effect, it is possible to greatly reduce the delay between the consumption/production of species and the detection of these events. This is because the magnetohydrodynamic force, through its action, quickly homogenizes the concentration of species in the solution.

$$F_B = j \times B \tag{1}$$

To address the current limitations and challenges inherent to the coupling of electrochemistry and NMR, a miniaturized system of composite electrodes was developed. The electrodes were prepared by mixing a graphite and expoxy (CaldoFix) resin. The choice in materials stems from the inherent limitation of using metallic electrodes in the detection region of the NMR spectrometer[6,19] as well as from the fact that
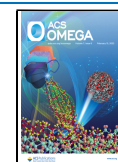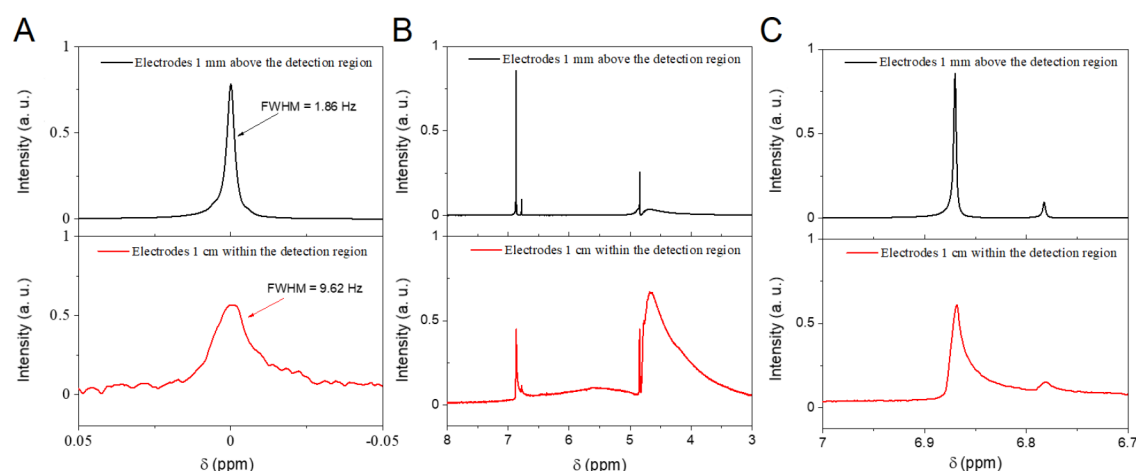
Figure 1. Evaluation of interference in the ^{1}H NMR spectra of benzoquinone due to the position of the electrodes. Black line: electrodes positioned 1 mm above the detection region. Red line: electrodes positioned 1 cm within the detection region. Signal attributed to (A) the standard TSPd4, (B) water, (C) benzoquinone and hydroquinone. A 0.05 mol·L^{-1} benzoquinone solution, after a 10 min long reaction, was used.

carbon-based electrodes can be used in a wide range of applications.[34−37] Furthermore, composite electrodes have been shown to have good mechanical stability, are able to withstand a wide range of applied potentials, and are compatible with nonaqueous solvents.[38−40] In addition, the electrode's surface can be renewed simply by polishing the material, which shows the advantages of using such electrodes and why their application in electrochemical systems has been investigated over the years.[38−41]

In this work we demonstrate the applicability of carbon−graphite composite electrodes (CGEEs) as an alternative that aids in reducing the challenges faced by the electrochemistry−NMR coupling. Both working and counter electrodes were miniaturized CGEEs, and they were used to analyze two electrochemical systems: the electro-reduction of bezoquinone and the electro-oxidation of isopropanol (ISP). Naturally, simultaneous observations of the systems were made using NMR; i.e., the experiments were performed in situ.

RESULTS AND DISCUSSION

The use of metallic electrodes for electrochemistry−NMR coupling causes several interference problems between the techniques, such as the increase in noise in electrochemical measurements and the loss of spectral quality in the NMR spectra.[6] Thus, a system of three miniaturized electrodes using mainly graphite and epoxy resin as raw materials was developed in order to minimize these issues. The applicability of this electrode system was evaluated by monitoring the reactions of electro-reduction of benzoquinone and electro-oxidation of the ISP in real time. In addition, the magneto-electrolysis effect was evaluated for both reactions. A great advantage of this approach is the possibility of replacing graphite with other carbon-based materials such as commercial catalysts with different percentages of nanoparticles or even by monitoring different electrochemical reactions (e.g., in fuel cells).

Benzoquinone Reduction. The study of the interference in the NMR spectra due to the positioning of the electrodes in the electrochemical cell relative to the detection region of the spectrometer was done by considering two positions: 1 mm above the detection region and 1 cm within it. For this analysis, the peaks of the TSPd4 standard, the water suppression region,

and the peaks corresponding to the analyte, benzoquinone, and the product, hydroquinone, were monitored. Figure 1 shows the spectra obtained in both conditions. Due to the fact that WE and CE were made from a composite of graphite and epoxy resin, it was expected that the insertion of these electrodes in the detection region would not significantly compromise the quality of the NMR spectrum. However, upon analysis of Figure 1, it was possible to verify that the homogeneity of the magnetic field was greatly compromised and, consequently, there was a broadening of all the peaks of the spectrum: the definition of the peak was lost (Figure 1 A, bottom) and the full width at half-maximum (fwhm) is much worse when the electrodes are inserted in the detection region (9.62 Hz) compared to when the electrodes are placed 1 mm above it (1.86 Hz), the suppression of the solvent signal was severely impaired (Figure 1 B) and the separation of the peaks referring to benzoquinone and hydroquinone was lost (Figure 1 C). This could be due to the fact that copper wires were used to make the electric contact with the electrodes and that this contact point was placed near the detection region. Another explanation could be that while graphite is not as magnetically active as some metals, it still has a much higher magnetic susceptibility than water, which changes the magnetic field distribution in its vicinity. With this in mind, the position chosen for electrodes was 1 mm above the detection region, since the magnetic force promotes homogenization of the sample due to the convection caused by this force.[19,33] Thus, it was possible to maintain the quality of NMR measurements.

The voltammetric profiles corresponding to the redox processes of benzoquinone in the presence and in the absence of the magnetic field are shown in Figure 2. The changes observed in these results are mainly due to the presence of the magnetic field, since the convection generated by the magnetic force takes more molecules of benzoquinone to the electrode, increasing the cathodic current, and the formed hydroquinone molecules quickly diffuse to the bulk of the solution, reducing the anodic current.[30] In the cathodic branch, referring to the reduction of benzoquinone, the peak potential changes from −0.38 V (ex situ) to somewhere around −0.80 V (in situ), where the peak actually becomes less defined. The cathodic peak currents were −0.11 mA (ex situ) and −0.44 mA (in situ). Thus, it was found that the cathodic current was about 4
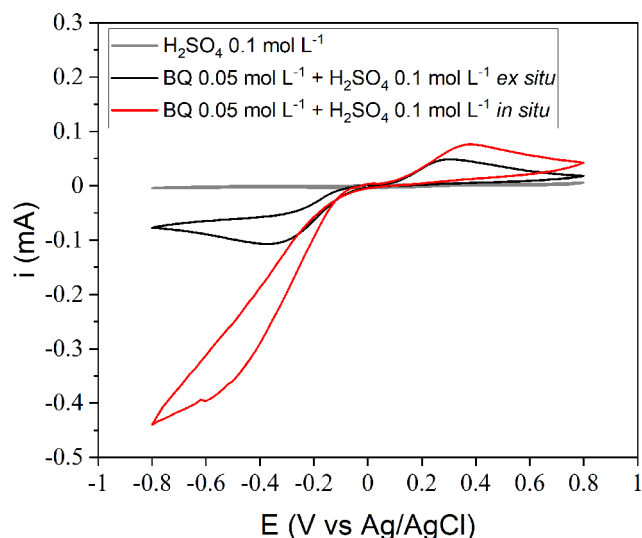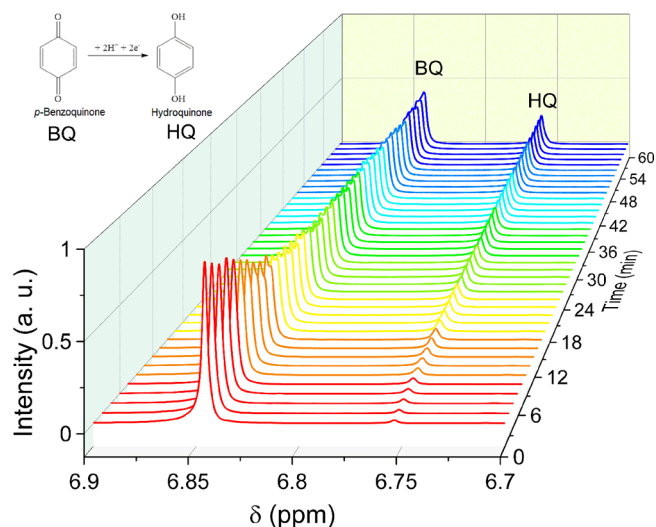
Figure 2. Cyclic voltamograms acquired, using graphite−epoxy composite electrodes, in situ (red line) and ex situ (black line).

Figure 4. ¹H spectrum of in situ reduction of benzoquinone, performed for 1 h.

times greater when the reaction was carried out in the presence of the magnetic field.

The chronoamperograms obtained during in situ and ex situ measurements with a fixed potential of −0.50 V (vs Ag/AgCl) are shown in Figure 3A). The analysis of the chronoamperograms reveals differences in the current magnitudes obtained in the different experimental conditions: during the ex situ measurement the cathodic current remained close to −0.1 mA, while in the in situ measurement, this parameter remained between −0.3 and −0.4 mA, in agreement with the results obtained by cyclic voltammetry. In addition to changes in the magnitude of the current, it is possible to observe that the current never stabilized during the in situ measurements, possibly due to the experimental configuration, where a turbulent flow may be formed in between the electrodes due to the relative orientations of the ion flow and the magnetic field (Figure 3B).

Figure 4 shows the ¹H NMR spectra obtained in situ during WE polarization at a potential of −0.5 V vs Ag/AgCl, for the electro-reduction of benzoquinone to hydroquinone. The peak

corresponding to benzoquinone diminishes in amplitude over time, as it is reduced while, conversely, the peak of hydroquinone increases in amplitude over time, as it is being formed. In addition, there is also a slight widening of the signal referring to the ¹H of benzoquinone during the in situ monitoring. However, the separation between the peaks was not compromised, which made it possible to quantify both species by their respective peak areas (Figure 5).

Figure 5 shows the ratio between the benzoquinone/hydroquinone peak area and the total spectrum area, R_S (eq 2), during both in situ and ex situ experiments. The points acquired in situ are represented by the filled squares with benzoquinone in black and hydroquinone in blue, and those acquired ex situ are represented by the white-filled squares. The data show a consumption of 26.7% of the initial benzoquinone and the formation of the same amount of hydroquinone when the reaction was carried out inside the 14 T NMR spectrometer. However, when this reaction was carried out outside the spectrometer, under the same concentration and temperature conditions, the amount of benzoquinone consumed corresponded to only 5.6% of the
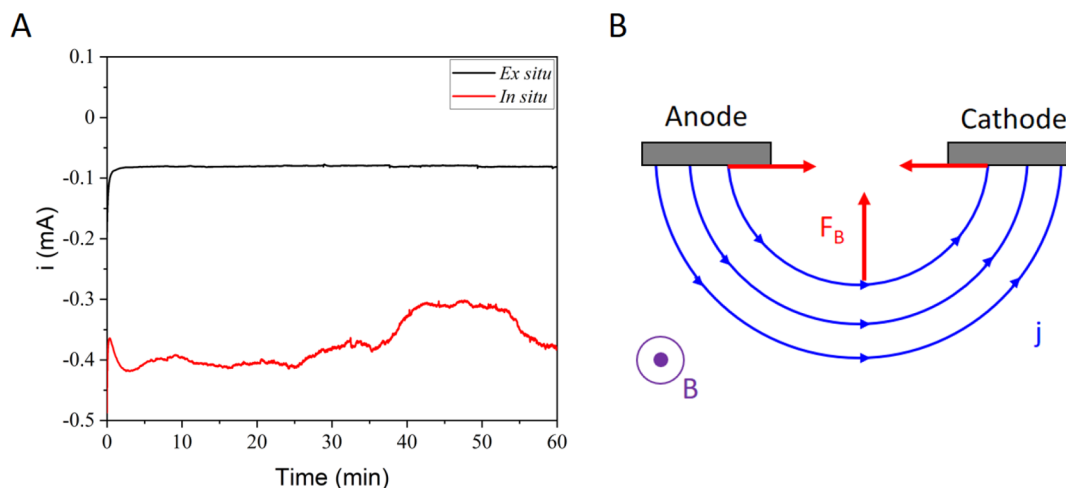
Figure 3. (A) Chronoamperograms acquired during measurements, using the composite graphite−epoxy electrodes, in situ (red line) and ex situ (black line) electrodes. (B) Relative orientation of the magnetic field, **B**, current density, **j**, and resulting magnetic force, **F$_B$**.
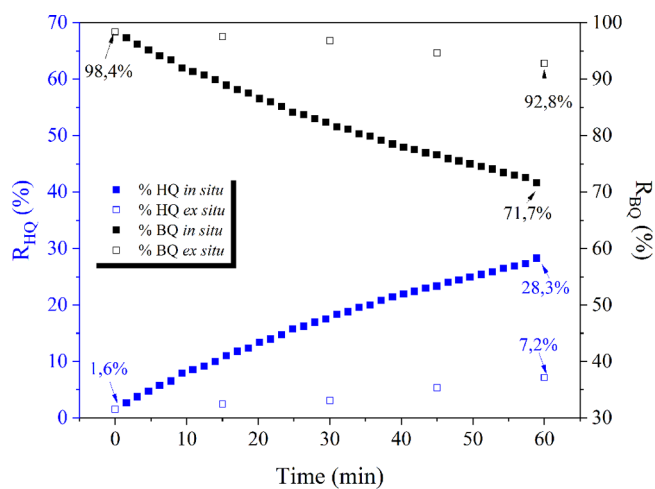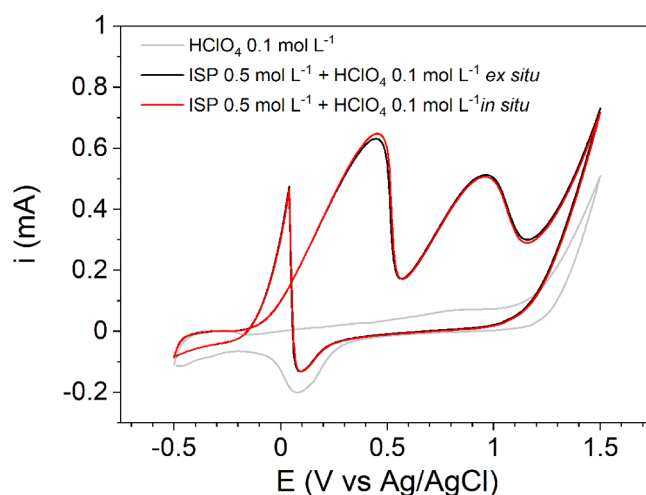
Figure 5. Percentage of area over time, of the in situ reduction of benzoquinone, of each ^{1}H peak of benzoquinone and of hydroquinone for 1 h.

Figure 6. Cyclic voltamograms acquired using the platinized composite graphite−epoxy electrode in situ (red) and ex situ (black) for the ISP electro-oxidation. The cycles shown are number 10 out of 10 acquired.

initial concentration. That is, the data obtained by high resolution NMR spectroscopy confirm the electrochemical data, showing that the reaction happens more quickly in the presence of the magnetic field of the spectrometer (approximately 4 times faster).

The set of results obtained from the in situ monitoring of the reduction of benzoquinone using the composite graphite−epoxy electrodes demonstrates their applicability during the electrochemistry−NMR coupling. Despite the small electroactive area of these electrodes, it was possible to convert around 25% of the benzoquinone into hydroquinone. However, the quality of the NMR spectra was somewhat compromised during the in situ monitoring of the electrochemical reaction, which was observed by the enlargement and a small distortion of the peaks referring to benzoquinone, at 6.85 ppm. This distortion, however, was not enough to compromise the quantitative measurements, given that both NMR and electrochemical results are in good agreement.

Isopropanol Oxidation. The electro-oxidation reaction of isopropanol, ISP, was monitored in situ to demonstrate the versatility of the graphite−epoxy composite electrodes. This reaction was chosen to be monitored in real time as it has great importance in the field of fuel cells,[42] in addition to its main reaction product, acetone, being easily identifiable by ^{1}H NMR, as it only displays a corresponding signal at 2.2 ppm. For this study, however, it was necessary to modify the working electrode to facilitate the reaction. The WE was modified through the electrodeposition of Pt and the voltammetric profile confirming the presence of Pt on the surface of the WE is shown by the gray line in Figure 6, where the Pt reduction peak occurs at around +0.12 V (vs Ag/AgCl). This figure also shows the cyclic voltamograms corresponding to the in situ and ex situ electrooxidation of ISP, red and black lines, respectively. The anodic scan of this voltamogram has two bands: the first one, whose maximum current is obtained at +0.45 V (versus Ag/AgCl), appears due to the dehydrogenation of the ISP, while the second band at +0.90 V corresponds to the bulk oxidation of 2-propanol.[43] In addition, the cathodic scan also has a band at +0.1 V vs Ag/AgCl due to the reactivation current of the catalyst (Pt black).

In the case of the ISP electro-oxidation reaction, the voltammetric results obtained in situ and ex situ were very

similar. A possible explanation for this observation is that the maximum oxidation current of alcohols is normally dependent on the formation of Pt oxides and not on the alcohol diffusion.[44] Thus, even with the effect of magnetoelectrolysis contributing to an increase in mass transport, it was not possible to observe a significant change in the voltammetric profile obtained in situ. In view of the similarity between the cyclic voltammograms acquired in situ and ex situ, real-time ^{1}H NMR measurements for the electro-oxidation of the ISP were only performed in situ.

Figure 7 shows the chronoamperogram corresponding to the oxidation of the ISP in the presence of the magnetic field. Due
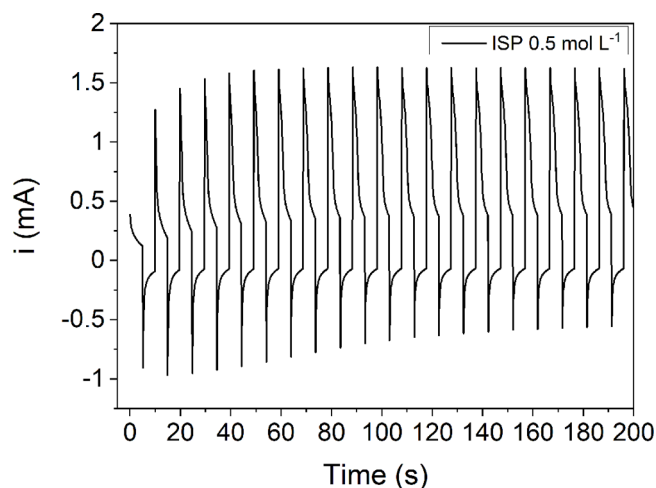
Figure 7. In situ chronoamperogram of the ISP oxidation using the electrochemical cell made with graphite and epoxy resin electrodes. The applied potential was +0.45 V vs Ag/AgCl, while the cleaning potential was −0.5 V vs Ag/AgCl. Both were applied sequentially for 5 s.

to the adsorption of organic molecules on the electrode surface, the catalytically active sites are blocked causing a decrease in the oxidation current. For this reason, it was necessary to periodically clean the electrode surface by applying a potential of −0.5 V (vs Ag/AgCl) to reactivate
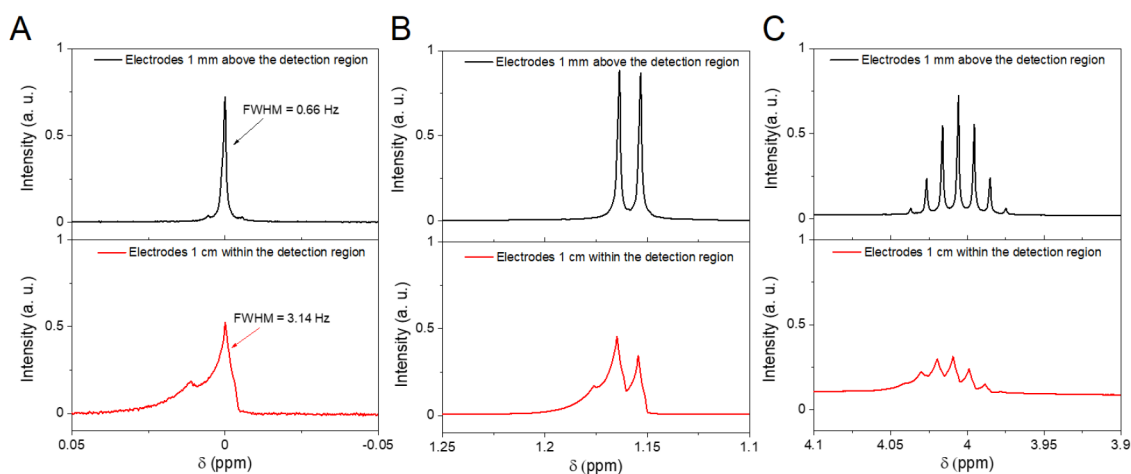
Figure 8. Evaluation of interference in the ^1H NMR spectra of isopropanol due to the position of the electrodes. The electrodes were positioned 1 mm above (black lines) and 1 cm within (red lines) the detection region. Signal referring to (A) the standard TSPd4, (B) ISP doublet, and (C) ISP multiplet.

the electrode surface and prevent the equilibrium current from being achieved so quickly. The applied potential was chosen because this experimental condition favors the formation of acetone.

Measured current density values (considering a geometric area of 7.9×10^{-3} cm^2, $j_{+0.45V}$ = 76 mA cm^{-2}) are in the same range as literature values obtained for the isopropanol electroxidation reaction.[45] The electrochemically active surface area (ECSA) was calculated using the hydrogen underpotential region (H_{upd}, integrated from −0.4 to −0.15 V) and was found to be 110 cm^2.

The influence of the platinum graphite−epoxy composite electrode's placement on the in situ monitoring of the ISP electro-oxidation was verified (Figure 8). Just as in the case of benzoquinone reduction, the insertion of the electrodes in the detection region also compromised the NMR spectral quality. Thus, taking advantage of the agitation generated by the presence of the electric current and the magnetic field, the electrodes were kept just 1 mm above the detection region, since in these conditions the NMR signals were very well-defined and the standard signal had a FWHM of 0.66 Hz (Figure 8a).

The resonance spectra obtained before and after the oxidation of ISP as well as the correspondence of the observed ^1H NMR signals are shown in Figure 9. The peaks H_a and H_b are characteristic of ISP. H_a are the hydrogen atoms of the methyl groups, while H_b is the hydrogen bonded to the central carbon atom. H_a produce a doublet signal in the NMR spectrum, with an area 6 times larger than the multiplet signal of H_b, just as expected by their ratio within the ISP molecule. H_c, meanwhile, are the hydrogen atoms of acetone, which, due to their equivalent chemical environment, produce a singlet in the NMR spectrum.

Figure 10 shows the regions of the ^1H NMR spectra corresponding to the peaks H_a (Figure 10a) and H_c (Figure 10b) acquired during the in situ oxidation of ISP. It is immediately clear from the figures that the spectral quality did not deteriorate over time, given that the FWHM of the peaks remains constant and no unfolding of the peaks was observed. As seen in Figure 11, the R_S of H_a decreases over time, owing to the consumption of ISP, and conversely, the R_S of H_c increases over time, due to the formation of acetone. More
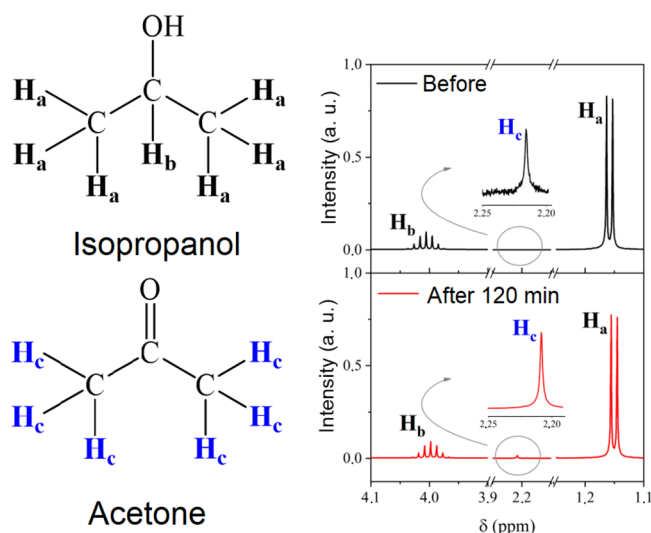

Figure 9. NMR spectra obtained in situ using platinum−graphite epoxy composite electrodes, before the reaction (black line) and after 120 min (red line) of ISP oxidation. The peaks for each ^1H nucleus are assigned in both spectra.

concretely, it was determined that only 1.6% of the ISP had been consumed after 2 h while the concentration of acetone increased by the same amount. The peak corresponding to H_b was not used for the determination of ISP concentration due to its proximity to the solvent signal (H_2O + D_2O) which, while not shown in Figure 9, is still close enough to influence the area of H_b. In addition, the peaks H_a and H_c correspond to the same number of hydrogen atoms and thus have a 1:1 ratio, which facilitated the comparison.

The data shown demonstrate that graphite−epoxy composite electrodes are adequate for monitoring the electro-reduction of ISP in real time if the electrodes are placed 1 mm above the NMR detection region. However, due to the small surface area of the WE, the amount of ISP consumed and, consequently, the amount of acetone formed was very small, even after 2 h of reaction.

Comparison with Other Setups. Table 1 shows a summary of the main characteristics of some setups used for in situ coupling between NMR and electrochemistry. More
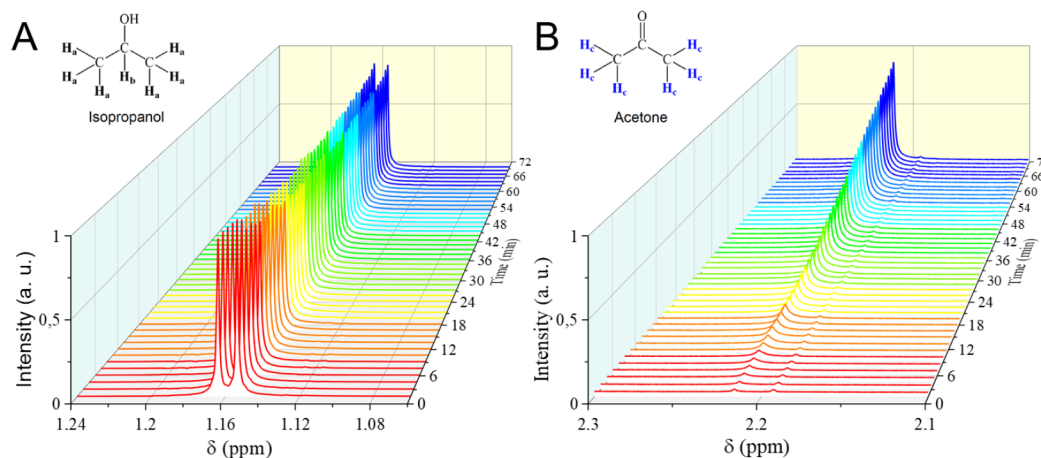
Figure 10. ^{1}H spectra of in situ ISP oxidation over a 120 min long reaction using the composite graphite−epoxy platinized electrodes. ISP concentration was 0.5 mol·L^{-1} in HClO$_4$ (0.1 mol·L^{-1}). (A) ISP consumption and (B) formation of acetone.
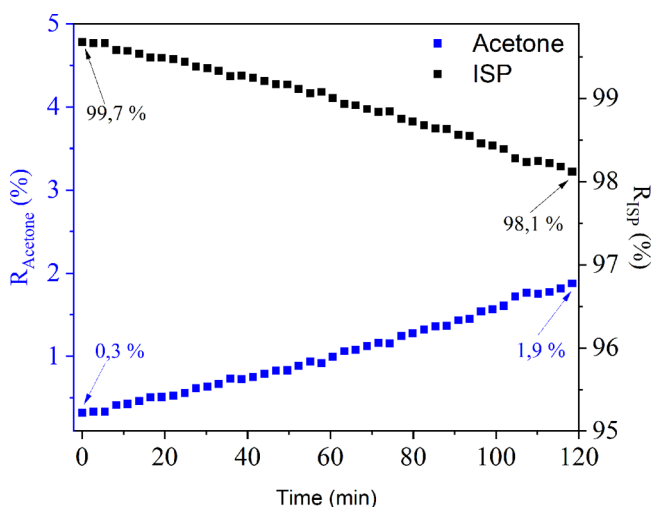
Figure 11. Graph of the percentage of area with time for in situ ISP oxidation. The areas correspond to the peaks referring to the hydrogens H$_a$ (black line) and H$_c$ (blue line). The former corresponding to the ISP doublet and the latter to the acetone singlet, during 120 min reaction.

information on current developments in the area of coupling between electrochemistry and liquid NMR can be found in the recent review published in 2021 by Pietrzak et al.[46]

■ CONCLUSIONS

The versatility of the developed cell was demonstrated with the monitoring of the electro-reduction of benzoquinone and the electro-oxidation of isopropanol both in situ and ex situ. It was possible to keep track of the consumption of the reagents and their respective products in real time. However, the percentage of ISP consumed in situ, 1.6%, was significantly lower than the percentage of benzoquinone consumed in situ, 26.7%, even with the platinum modification of the electrode for the alcohol oxidation.

The highlights of the developed graphite−epoxy-based electrodes are the simplicity of their fabrication and their low cost, with the added benefit that both the support material and the catalyst can be modified to suit the desired application. However, there are still some limitations regarding the positioning of the electrode relative to the detection region of the NMR spectrometer and the electrochemical current generated and supported by this system. Regarding the restriction of placing these electrodes inside the NMR detection region, the magnetoelectrolysis effect can be taken advantage of to increase the homogeneization rate of the sample solution during the in situ reaction, thus reducing the time between product formation and its detection. However, this effect must also be kept in mind, evaluated, and considered during the comparisons between in situ and ex situ experimental results. As a final note, this type of electrode is recommended for researchers who are starting their work with

Table 1. Comparison of Miniaturized Electrodes for EC−NMR Coupling

	carbon fiber electrode[2,19]	metallic wire electrode[5,19]	graphite−epoxi electrode
costs	low	low, metal can be reused	low, disposable electrodes
modification of the electrode surface	It is possible, but the attachment of other materials to the fiber is difficult.	Different metals can be used (e.g., Pt, Pd, Au, etc.).	Different materials can be used (e.g., carbon supported catalysts, etc.).
application for different analytes	Although electrochemically resistant, it can be applied to a limited range of analytes when not modified.	broad	broad
NMR probe modifications required?	no	no	no
large surface area	yes, but difficult to quantify the geometric area	yes, and it can be improved by increasing the superficial roughness of the material	It depends on the support material used and the surface modification.
can be inserted in detection region?	yes	no	no

coupling electrochemistry and NMR and who want to build their own electrodes.

EXPERIMENTAL SECTION

Chemicals and Solutions. *Benzoquine Electro-reduction.* *p*-Benzoquinone (98% purity) and D_2O were acquired from Sigma-Aldrich, and H_2SO_4 (95% purity) was acquired from Vetec. Prior to electrochemical experiments, *p*-benzoquinone was disolved in hot water ($T = 70$ °C) and stirred for 30 min, after which the solution was allowed to cool down to 25 °C and filtered to obtain pure recrystallized *p*-benzoquinone (this was confirmed by ^{1}NMR). The analyte solution, containing 0.05 mol·L^{-1} of *p*-benzoquinone, was prepared in ultrapure water (18.2 MΩ·cm) and the pH was adjusted to 1 using H_2SO_4, which corresponds to a concentration of 0.1 mol·L^{-1} (supporting electrolyte).

Isopropanol Electro-oxidation. Isopropanol (98% purity), perchloric acid (70% purity), chloroplatinic acid (37.5% purity), lead acetate (95% purity),and deuterated water, D_2O, were all obtained from Sigma-Aldrich. The supporting electrolyte was a 0.1 mol·L^{-1} $HClO_4$ solution . The analyte solution used in the electrochemical experiments was prepared in the supporting electrolyte solution and contained 0.5 mol·L^{-1} isopropanol.

For both the benzoquinone and isopropanol reactions, the total volume of the solution used was 660 μL, with 60 μL of D_2O being diluted in 600 μL of the analyte solution.

To platinize the working electrode, a solution containing 0.02 mol·L^{-1} chloroplatinic acid and 3.2×10^{-5} mol·L^{-1} lead acetate was used.

Electrochemical Cell and Measurement Devices. *Apparatus.* Electrochemical measurements were performed with an EmStat2 potentiostat (Utrecht, The Netherlands). ^{1}H NMR experiments were carried out in a 600 MHz NMR spectrometer (Ascend 600 Bruker).

Glass Capillaries. Commercial glass capillaries with a volume of 100 μL, of 5.9 and 12.5 cm in height for the reference and for the WE and CE, respectively, from Blaubrand were used to make the electrodes.

Electrochemical Cell. The cell developed to monitor the electro-reduction reaction of benzoquinone and the electro-oxidation of the ISP consisted of a system of three electrodes in a 5 mm NMR tube, as shown in Figure 12.
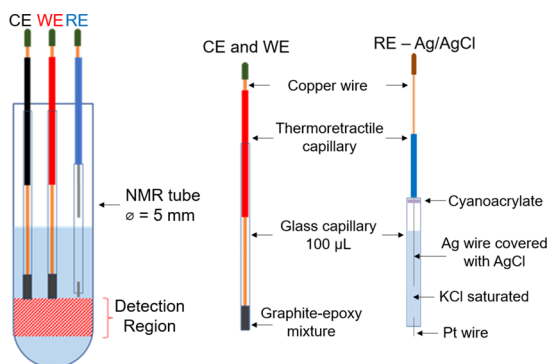
Figure 12. Electrochemical cell illustration. The cell was built in an NMR tube with a 5 mm outer diameter. The cell is not to scale. WE, CE, and RE refer to the working, counter, and reference electrodes, respectively.

The working electrode (WE) and the counter electrode (CE) were prepared with a mixture of graphite and epoxy resin (Caldofix) in a 3:1 mass ratio, respectively, mixed under mechanical agitation until the mixture was completely homogeneous (mixing lasted around 5 min). This paste was compacted inside a commercial 100 μL glass capillary with a height of 12.5 cm. The electrical contact with the graphite paste was made before the resin was cured, which requires at least 24 h, with a 0.5 mm thick copper wire inserted at the opposite end of the capillary (see Figure 12). The reference electrode (RE) consisted of a miniaturized Ag/AgCl electrode. This electrode was built in a 100 μL capillary with a height of 5.9 cm. A Pt wire was fixed at one end of the glass capillary by melting the glass and it was filled with a KCl-saturated aqueous solution (between half and one centimeter of the Pt wire were left both inside and outside the capillary). An AgCl film was electrodeposited on a properly cleaned 0.1 mm thick Ag wire which was then inserted in the solution-filled capillary. Finally, the Ag wire was fixed at the other end of the capillary using a cianoacrylate resin (superglue). No modification of the WE surface was needed to perfom the benzoquinone reduction reaction; however, the electrode surface was platinized to monitor the isopropanol oxidation reaction. To platinize the graphite—epoxy electrode surface, a potential of −1 V vs Ag/AgCl was applied for 10 min with the electrode being placed in a chloroplatinic acid solution.

Electrical Connections. The electrochemical cell was connected to the potentiostat via a triple cable with a protective copper mesh. Halfway between the cell and the potentiostat, chokes (inductors with a 200 μH inductance) were attached on each cable (i.e., there was one choke for each electrode). These were necessary to filter the noise signals that are introduced during the electrochemical measurements in the NMR spectra and vice versa.

Measurement Parameters. *Electrochemical Measurements.* Electrochemical measurements were performed using the cyclic voltammetry and chronoamperometry techniques. The parameters used for both techniques are described in Table 2. All electrodes used were rinsed with ultrapure water and preconditioned using 30 cyclic voltammetry cycles, in the respective supporting electrolyte.

The electrodes were positioned using the Bruker sampler, as illustrated in Figure 13. More details on how to position the electrodes inside the NMR tube and how the height in relation to the detection region was measured can be found in the tutorial video of the Supporting Information of ref 19.

Table 2. Electrochemical Parameters Used for the Benzoquinone Electro-reduction and Isopropanol Electro-oxidation

parameter	benzoquinone electro-reduction	isopropanol electro-oxidation
Cyclic Voltammetry		
potential range (V vs Ag/AgCl)	−0.8 to +0.8	−0.5 to +1.5
scan rate (mV s^{-1})	10	100
potential step (mV)	1.0	10
Chronoamperometry		
potential (V vs Ag/AgCl)	−0.5	+0.45 for 5 s and −0.5 for 5 s
duration (s)	3600	3600
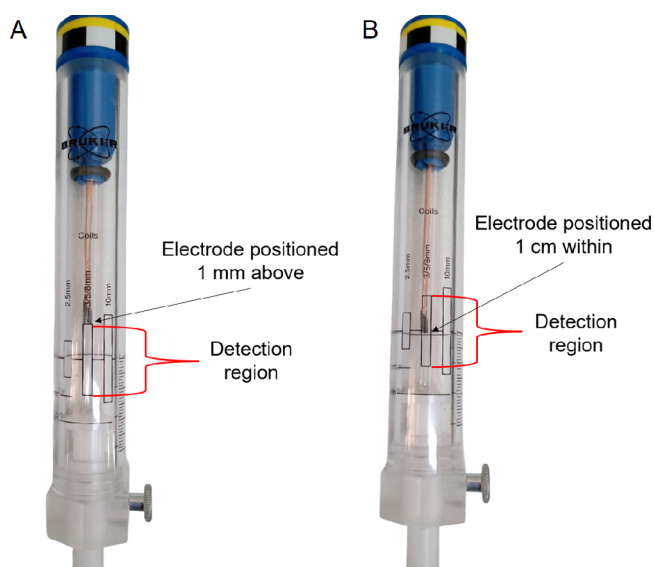
Figure 13. Adjustment of the height of the electrodes in relation to the NMR detection region using a standard Bruker accessory. (A) Electrode positioned 1 mm above the detection region. (B) Electrode positioned 1 cm within the detection region.

NMR Parameters and Sequences. Before the NMR measurements, the "shimming" was performed, which consists of adjusting the homogeneity of the magnetic field until the full width at half-maximum, FWHM, of the chosen standard was close to 1 Hz. The standard, TSPd4 (3-(trimethylsilyl)-propionic-2,2,3,3-d_4 acid sodium salt with a purity of 98%, acquired from Sigma-Aldrich), was mixed with the analyte solution, and the shimming was performed with the electrochemical cell in the NMR spectrometer. In addition, the 90° pulse was calibrated for each sample. All measurements were performed at a temperature of 25 °C.

Benzoquinone NMR Sequence Parameters. The zgpr sequence (Bruker standard) was used to monitor the BQ reduction reaction. The d1 recycling time was 5.00 s, the acquisition time (AQ) was 2.73 s, the number of dummy scans (DS) was 4, and the number of scans (NS) was 8. With these parameters the total acquisition time for each spectrum was 93 s.

Isopropanol NMR Sequence Parameters. The zg sequence (Bruker standard) was used to monitor the electro-oxidation of the ISP. The d1 recycling time was 5.00 s, the acquisition time (AQ) was 3.00 s, the number of dummy scans (DS) was 4, and the number of scans (NS) was 16. With these parameters the total acquisition time for each spectrum was 160 s.

The percentage of consumption of benzoquinone, and that of hydroquinone production was calculated as the ratio between the respective species' peak and the total NMR spectrum area, R_S, as shown in eq 2.

$$R_S = \frac{A_S}{A_{\text{reagent}} + A_{\text{product}}} \times 100\% \tag{2}$$

where A_S is the area of the peak belonging to species S, and A_{reagent} and A_{product} are the peak areas of reagent and product, respectively. In the case of benzoquinone electro-reduction, the reagent is benzoquinone and hydroquinone is the product, while for the electro-oxidation of isopropanol, isopropanol is the reagent and the product is acetone. All measurements were repeated a minimum of three times each, with the electrodes

maintaining a stable response during the one and a half hours that the experiments lasted. The electrodes were built to be disposable, so that a new and clean surface could be used in each experiment, thus avoiding any cross contamination.

All the experiments, in situ and ex situ, were carried out in the same spectrometer. The term in situ refers to the electrochemical reactions conducted inside the NMR spectrometer, while the ex situ measurements (control) were conducted outside the spectrometer, and the NMR spectra were acquired before and after the electrochemical reactions.

■ AUTHOR INFORMATION

Corresponding Author

Bruna Ferreira Gomes − *Instituto de Química de São Carlos, Universidade de São Paulo, 13566-590 São Carlos, SP, Brazil*; Present Address: Electrochemical Process Engineering, University of Bayreuth, Universitätsstraße 30, 95 447 Bayreuth, Germany; orcid.org/0000-0002-6879-3583; Email: bruna.lobo@uni-bayreuth.de

Authors

Pollyana Ferreira da Silva − *Instituto de Química de São Carlos, Universidade de São Paulo, 13566-590 São Carlos, SP, Brazil*

Carlos Manuel Silva Lobo − *Instituto de Química de São Carlos, Universidade de São Paulo, 13566-590 São Carlos, SP, Brazil*; Present Address: University of Stuttgart, Institute of Technical Chemistry, Pfaffenwaldring 55, 70 569 Stuttgart, Germany; orcid.org/0000-0002-7727-008X

Marcelo Carmo − *Forschungszentrum Jülich GmbH, 52428 Jülich, Germany*; orcid.org/0000-0002-0186-317X

Christina Roth − *Electrochemical Process Engineering, University of Bayreuth, 95447 Bayreuth, Germany*

Luiz Alberto Colnago − *Embrapa Instrumentação, 13560-970 São Carlos, SP, Brazil*

Complete contact information is available at:
https://pubs.acs.org/10.1021/acsomega.1c05823

Notes

The authors declare no competing financial interest.

■ ADDITIONAL NOTE

[a]Note that all quantities denoted in bold throughout this text represent vector quantities.

■ REFERENCES

(1) Richards, J.; Evans, D. Flow cell for electrolysis within the probe of a nuclear magnetic resonance spectrometer. *Anal. Chem.* **1975**, *47*, 964−966.

(2) Klod, S.; Ziegs, F.; Dunsch, L. In Situ NMR Spectroelectrochemistry of Higher Sensitivity by Large Scale Electrodes. *Anal. Chem.* **2009**, *81*, 10262−10267.

(3) Klod, S.; Haubner, K.; Jaehne, E.; Dunsch, L. Charge stabilisation by dimer formation of an endcapped thiophene tetramer-an in situ NMR spectroelectrochemical study. *Chem. Sci.* **2010**, *1*, 743−750.

(4) Klod, S.; Dunsch, L. A combination of in situ ESR and in situ NMR spectroelectrochemistry for mechanistic studies of electrode reactions: the case of p-benzoquinone. *Magn. Reson. Chem.* **2011**, *49*, 725−729.

(5) Webster, R. D. In situ electrochemical-NMR spectroscopy. Reduction of aromatic halides. *Anal. Chem.* **2004**, *76*, 1603−1610.

(6) Bussy, U.; Boujtita, M. Review of advances in coupling electrochemistry and liquid state NMR. *Talanta* **2015**, *136*, 155−160.

(7) Nunes, L. M. S.; Moraes, T. B.; Barbosa, L. L.; Mazo, L. H.; Colnago, L. A. Monitoring electrochemical reactions in situ using steady-state free precession C-13 NMR spectroscopy. *Anal. Chim. Acta* **2014**, *850*, 1−5.

(8) Evans, D. F. The determination of the paramagnetic susceptibility of substances in solution by nuclear magnetic resonance. *J. Chem. Soc.* **1959**, 2003.

(9) Prenzler, P. D.; Bramley, R.; Downing, S. R.; Heath, G. A. High-field NMR spectroelectrochemistry of spinning solutions: simultaneous in situ detection of electrogenerated species in a standard probe under potentiostatic control. *Electrochem. commun.* **2000**, *2*, 516−521.

(10) Mincey, D. W.; Popovich, M. J.; Faustino, P. J.; Hurst, M. M.; Caruso, J. A. Monitoring of electrochemical reactions by nuclear-magnetic-resonance spectrometry. *Anal. Chem.* **1990**, *62*, 1197−1200.

(11) Bussy, U.; Giraudeau, P.; Tea, I.; Boujtita, M. Understanding the degradation of electrochemically-generated reactive drug metabolites by quantitative NMR. *Talanta* **2013**, *116*, 554−558.

(12) Bhattacharyya, R.; Key, B.; Chen, H.; Best, A. S.; Hollenkamp, A. F.; Grey, C. P. In situ NMR observation of the formation of metallic lithium microstructures in lithium batteries. *Nat. Mater.* **2010**, *9*, 504−510.

(13) Trease, N. M.; Köster, T. K. J.; Grey, C. P. In situ NMR Studies of Lithium Ion Batteries. *J. Electrochem. Soc. Interface* **2011**, *20*, 69−73.

(14) Trease, N. M.; Zhou, L. N.; Chang, H. J.; Zhu, B. Y. X.; Grey, C. P. In situ NMR of lithium ion batteries: Bulk susceptibility effects and practical considerations. *Solid State Nucl. Magn. Reson.* **2012**, *42*, 62−70.

(15) Rapta, P.; Zeika, O.; Rohde, D.; Hartmann, H.; Dunsch, L. Thiophene-thiophene versus phenyl-phenyl coupling in 2-(diphenylamino)-thiophenes: An ESR-UV/Vis/NIR spectroelectrochemical study. *ChemPhysChem* **2006**, *7*, 863−870 14.

(16) Klett, M.; Giesecke, M.; Nyman, A.; Hallberg, F.; Lindstrom, R. W.; Lindbergh, G.; Furo, I. Quantifying Mass Transport during Polarization in a Li Ion Battery Electrolyte by in Situ Li-7 NMR Imaging. *J. Am. Chem. Soc.* **2012**, *134*, 14654−14657.

(17) Harks, P. P. R. M. L.; Mulder, F. M.; Notten, P. H. L. In situ methods for Li-ion battery research: A review of recent developments. *J. Power Sources* **2015**, *288*, 92−105.

(18) Krachkovskiy, S. A.; Bazak, J. D.; Werhun, P.; Balcom, B. J.; Halalay, I. C.; Goward, G. R. Visualization of Steady-State Ionic Concentration Profiles Formed in Electrolytes during Li-Ion Battery Operation and Determination of Mass-Transport Properties by in Situ Magnetic Resonance Imaging. *J. Am. Chem. Soc.* **2016**, *138*, 7992−7999.

(19) Silva, P. F. d.; Gomes, B. F.; Lobo, C. M. S.; Queiroz Júnior, L. H. K.; Danieli, E.; Carmo, M.; Blümich, B.; Colnago, L. A. Electrochemical NMR spectroscopy: Electrode construction and magnetic sample stirring. *Microchem. J.* **2019**, *146*, 658−663.

(20) Monzon, L. M. A.; Klodt, L.; Coey, J. M. D. Nucleation and Electrochemical Growth of Zinc Crystals on Polyaniline Films. *J. Phys. Chem. C* **2012**, *116*, 18308−18317.

(21) Monzon, L. M. A.; Coey, J. M. D. Magnetic fields in electrochemistry: The Kelvin force. A mini-review. *Electrochem. commun.* **2014**, *42*, 42−45.

(22) Monzon, L. M. A.; Coey, J. M. D. Magnetic fields in electrochemistry: The Lorentz force. A mini-review. *Electrochem. commun.* **2014**, *42*, 38−41.

(23) Bund, A.; Koehler, S.; Kuehnlein, H. H.; Plieth, W. Magnetic field effects in electrochemical reactions. *Electrochim. Acta* **2003**, *49*, 147−152.

(24) Bund, A.; Kuehnlein, H. H. Role of magnetic forces in electrochemical reactions at microstructures. *J. Phys. Chem. B* **2005**, *109*, 19845−19850.

(25) Hinds, G.; Spada, F. E.; Coey, J. M. D.; Mhiochain, T. R. N.; Lyons, M. E. G. Magnetic field effects on copper electrolysis. *J. Phys. Chem. B* **2001**, *105*, 9487−9502.

(26) O'Reilly, C.; Hinds, G.; Coey, J. M. D. Effect of a magnetic field on electrodeposition - Chronoamperometry of Ag, Cu, Zn, and Bi. *J. Electrochem. Soc.* **2001**, *148*, C674−C678.

(27) Leventis, N.; Dass, A. Demonstration of the Elusive Concentration-Gradient Paramagnetic Force. *J. Am. Chem. Soc.* **2005**, *127*, 4988−4989.

(28) Gomes, B. F.; Nunes, L. M. S.; Lobo, C. M. S.; Cabeca, L. F.; Colnago, L. A. In Situ Study of the Magnetoelectrolysis Phenomenon during Copper Electrodeposition Using Time Domain NMR Relaxometry. *Anal. Chem.* **2014**, *86*, 9391−9393.

(29) Gomes, B. F.; Nunes, L. M. S.; Lobo, C. M. S.; Carvalho, A. S.; Cabeca, L. F.; Colnago, L. A. In situ analysis of copper electro-deposition reaction using unilateral NMR sensor. *J. Magn. Reson.* **2015**, *261*, 83−86.

(30) Ferreira Gomes, B.; Ferreira da Silva, P.; Silva Lobo, C. M.; da Silva Santos, M.; Colnago, L. A. Strong magnetoelectrolysis effect during electrochemical reaction monitored in situ by high-resolution NMR spectroscopy. *Anal. Chim. Acta* **2017**, *983*, 91−95.

(31) Ferreira Gomes, B.; Holzhauser, F. J.; Silva Lobo, C. M.; Ferreira da Silva, P.; Danieli, E.; Carmo, M.; Colnago, L. A.; Palkovits, S.; Palkovits, R.; Blumich, B. Sustainable Electrocoupling of the Biogenic Valeric Acid under in Situ Low-Field Nuclear Magnetic Resonance Conditions. *ACS Sustain. Chem. Eng.* **2019**, *7*, 18288−18296.

(32) Lobo, C. M. S.; Gomes, B. F.; Bouzouma, H.; Danieli, E.; Blümich, B.; Colnago, L. A. Improving in operando low field NMR copper electrodeposition analyses using inductively coupled coils. *Electrochim. Acta* **2019**, *298*, 844−851.

(33) Benders, S.; Gomes, B. F.; Carmo, M.; Colnago, L. A.; Blümich, B. In-situ MRI velocimetry of the magnetohydrodynamic effect in electrochemical cells. *J. Magn. Reson.* **2020**, *312*, 106692.

(34) Manea, F.; Radovan, C.; Pop, A.; Corb, I.; Burtica, G.; Malchev, P.; Picken, S.; Schoonman, J. *Carbon Composite Electrodes Applied for Electrochemical Sensors. Sensors for Environment, Health and Security*; Dordrecht, 2009; pp 179−189.

(35) McCreery, R. L. Advanced Carbon Electrode Materials for Molecular Electrochemistry. *Chem. Rev.* **2008**, *108*, 2646−2687.

(36) Uslu, B.; Ozkan, S. A. Electroanalytical Application of Carbon Based Electrodes to the Pharmaceuticals. *Anal. Lett.* **2007**, *40*, 817−853.

(37) Wei, Z. D.; Ji, M. B.; Chen, S. G.; Liu, Y.; Sun, C. X.; Yin, G. Z.; Shen, P. K.; Chan, S. H. Water electrolysis on carbon electrodes enhanced by surfactant. *Electrochim. Acta* **2007**, *52*, 3323−3329.

(38) Chang, M.-L.; Chang, C.-M. Voltammetric determination of sunscreen by convenient epoxy-carbon composite electrodes. *J. Food Drug Anal.* **2001**, *9*, 7.

(39) Corb, I.; Manea, F.; Radovan, C.; Pop, A.; Burtica, G.; Malchev, P.; Picken, S.; Schoonman, J. Carbon-based Composite Electrodes: Preparation, Characterization and Application in Electroanalysis. *Sensors* **2007**, *7*, 2626.

(40) Pumera, M.; Merkoçi, A.; Alegret, S. Carbon nanotube-epoxy composites for electrochemical sensing. *Sens Actuators B Chem.* **2006**, *113*, 617−622.

(41) Borenstein, A.; Hanna, O.; Attias, R.; Luski, S.; Brousse, T.; Aurbach, D. Carbon-based composite materials for supercapacitor electrodes: a review. *J. Mater. Chem. A* **2017**, *5*, 12653−12672.
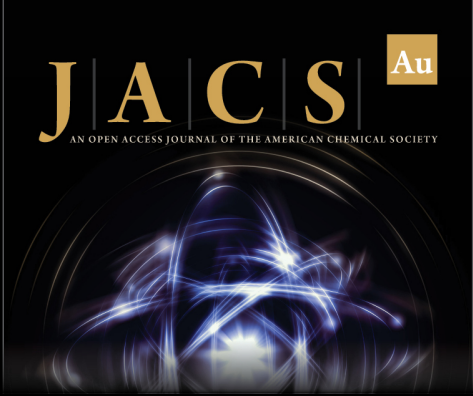
(42) Hauenstein, P.; Seeberger, D.; Wasserscheid, P.; Thiele, S. High performance direct organic fuel cell using the acetone/isopropanol liquid organic hydrogen carrier system. *Electrochem. commun.* **2020**, *118*, 106786.

(43) Rodrigues, I. A.; De Souza, J. P. I.; Pastor, E.; Nart, F. C. Cleavage of the C-C Bond during the Electrooxidation of 1-Propanol and 1-Propanol: Effect of the Pt Morphology and of Codeposited Ru. *Langmuir* **1997**, *13*, 6829−6835.

(44) Puthiyapura, V. K.; Lin, W.-F.; Russell, A. E.; Brett, D. J. L.; Hardacre, C. Effect of Mass Transport on the Electrochemical Oxidation of Alcohols Over Electrodeposited Film and Carbon-Supported Pt Electrodes. *Top. Catal.* **2018**, *61*, 240−253.

(45) Waidhas, F.; Haschke, S.; Khanipour, P.; Fromm, L.; Görling, A.; Bachmann, J.; Katsounaros, I.; Mayrhofer, K. J. J.; Brummel, O.; Libuda, J. Secondary Alcohols as Rechargeable Electrofuels: Electro-oxidation of Isopropyl Alcohol at Pt Electrodes. *ACS Catal.* **2020**, *10*, 6831−6842.

(46) Pietrzak, M.; Jopa, S.; Mames, A.; Urbańczyk, M.; Woźny, M.; Ratajczyk, T. Recent Progress in Liquid State Electrochemistry Coupled with NMR Spectroscopy. *ChemElectroChem.* **2021**, *8*, 4181−4198.